Nuclear Instruments and Methods in Physics Research A 705 (2013) 74–84

Contents lists available at SciVerse ScienceDirect

Nuclear Instruments and Methods in Physics Research A

journal homepage: www.elsevier.com/locate/nima

The wavelength frame multiplication chopper system for the ESS test beamline at the BER II reactor—A concept study of a fundamental ESS instrument principle

M. Strobl [a,b,*], M. Bulat [a], K. Habicht [a]

[a] Helmholtz Zentrum Berlin für Materialien und Energie, Hahn-Meitner-Platz 1, 14109 Berlin, Germany
[b] European Spallation Source ESS-AB, Tunavägen 24, 22100 Lund, Sweden

ARTICLE INFO

Article history:
Received 12 September 2012
Received in revised form
10 November 2012
Accepted 20 November 2012
Available online 21 December 2012

Keywords:
Neutron physics
Neutron instrumentation
Chopper systems
Wavelength frame multipliation

ABSTRACT

Contributing to the design update phase of the European Spallation Source ESS–scheduled to start operation in 2019–a test beamline is under construction at the BER II research reactor at Helmholtz Zentrum Berlin (HZB). This beamline offers experimental test capabilities of instrument concepts viable for the ESS. The experiments envisaged at this dedicated beamline comprise testing of components as well as of novel experimental approaches and methods taking advantage of the long pulse characteristic of the ESS source. Therefore the test beamline will be equipped with a sophisticated chopper system that provides the specific time structure of the ESS and enables variable wavelength resolutions via wavelength frame multiplication (WFM), a fundamental instrument concept beneficial for a number of instruments at ESS. We describe the unique chopper system developed for these purposes, which allows constant wavelength resolution for a wide wavelength band. Furthermore we discuss the implications for the conceptual design for related instrumentation at the ESS.

1. Introduction

The 5 MW ESS long pulse spallation source [1–3] will be the neutron source with the brightest peak flux available, delivering neutron pulses with a frequency of 14 Hz and a burst time of 2.86 ms. The time averaged flux will be comparable to the flux of the best continuous high flux reactor neutron sources [4–6]. In contrast to the most powerful short pulse sources like the Spallation Neutron Source (SNS) in the US [7] and the Japanese Spallation Neutron Source at J-PARC [8] the long pulse source offers the possibility to tune the resolution function even for white beam time-of-flight instruments [9–14], while the wavelength resolution is defined and fixed by the burst time and the instrument length at short pulse sources. The long pulses allow for highly efficient instrumentation for large scale structure instrumentation such as SANS, reflectometry and spin-echo spectroscopy, all requiring relaxed wavelength resolution of about 10% for the majority of applications [14]. However, not only different methods but also individual measurements e.g. in neutron reflectometry are most efficient when the resolution can be tuned to the requirements of a particular experiment [15–20]. Furthermore for the latter applications a broad, simultaneously covered wavelength band is advantageous because it allows for accessing a broad q-range (energy range) simultaneously in time resolved studies. Instruments at a pulsed source have to be kept short in order to provide such conditions. However, to still achieve or to tune to desired wavelength resolutions, wavelength frame multiplication (WFM) has been proposed [9–11,21,22] as a method for long pulse target stations and shown to be feasible by proof-of-principle experiments [12,13].

During the current design update phase of the ESS project a test beamline is under construction at the Helmholtz Zentrum-Berlin as part of the German in-kind contribution. This test beamline shall enable a large number of experiments and measurements of specific components required for ESS instruments as well as prototypes of detectors, broad band polarization devices, choppers or even special mechanical components, e.g. fast changing collimation systems. In particular the beamline will provide the opportunity to develop and test methodical approaches for ESS instruments.

In order to serve tests and methods with different wavelength resolution conditions, the test beamline must simulate the time structure of the ESS source on one hand and requires an advanced and flexible WFM chopper system on the other hand. Consequently the test beamline provides choppers mimicking the specific time structure expected at the ESS as well as choppers

* Corresponding author at: European Spallation Source ESS-AB, P.O. Box 176, Tunavägen 24, 221 00 Lund, Sweden.
Tel.: +46 721 79 20 68; fax: +46 46 888 30 68.
E-mail address: markus.strobl@esss.se (M. Strobl).

0168-9002/$ - see front matter © 2012 Elsevier B.V. All rights reserved.
http://dx.doi.org/10.1016/j.nima.2012.11.190

to adjust the wavelength resolution in a WFM mode. Given the ESS pulse structure, wavelength frame multiplication will be realized just like those in a number of proposed ESS instruments. Consequently the chopper system at the test beamline constitutes a real experimental test case for future ESS instrumentation.

In the following the basic beamline parameters are outlined. We then describe in detail the conceptual design of the full chopper system. Finally we discuss important conclusions valuable for related concepts at ESS.

2. ESS test beamline at HZB

The guide system in the neutron guide hall 1 at HZB has been subject to an extensive upgrade program, including an upgrade of several instruments [23,24]. In the course of this program, instruments were relocated, optimizing their positions, which also allowed installing an additional neutron guide. This guide now hosting the ESS test beamline directly views the center of the new HZB cold source and is located between the neutron guides for the renewed cold neutron TOF spectrometer (NEAT) [23] and the SANS instrument V4 [25]. The beamline consists of a 46.17 m long super-mirror coated guide providing 3 times larger angles of total reflection ($m=3$) than a Ni coated guide. The guide has a large cross-section of 60×125 mm^2. The guide system (see Fig. 1) starts at a distance of 1.53 m from the cold source with an in-pile section feeding in total 6 guides (1.87 m length). From there the guide separates from the common section with its final width of 60 mm being straight for the following 1.53 m, where a rotary shutter is installed. The following 5 m are curved with a radius of curvature $R_{C1}=1500$ m followed by another 30.45 m long curved section with a radius of $R_{C2}=2300$ m.The final 5 m long section is straight and ends at 46.17 m from the cold source. In order to host choppers the guide system provides several gaps: a 15 cm gap at 21.7 m, a 25 cm gap at 31.5 m and 10 cm gaps each at 30.4 m and 37.6 m from the cold source. An additional large 0.6 m gap provides space for the WFM pulse shaping choppers (PSC) at 28.3 m–28.9 m from the cold source. The curvature and the $m=3$ coating result in a spectrum with a cut-off wavelength of about 2 Å (Fig. 2). The guide ends close to the SANS detector vessel providing approximately 1 m space between the vessel, and the shielding of the NEAT guide system, which increases to 2 m at the end of the guide hall 14 m downstream (60 m from the cold source).

2.1. Source chopper system

A long pulse from a neutron spallation source as planned for the ESS has a distinguished pulse shape [26]. In contrast to short pulse sources having a sharp peak the pulse brightness rises steeply and then slowly reaches a plateau. The long tail which follows either the plateau in the case of the long pulse or the peak in the case of the short pulse is determined mainly by the moderator properties and is comparable in both cases. In order to mimic such long pulse structure a double chopper system is well suited. The characteristic rise, which is first steep and then slower, is achieved by two different chopper speeds. One chopper opens fast, the second one delays the full opening of the beam and the plateau is reached when both choppers are fully open. However, the long tail cannot be mimicked with a combination of trapezoidal transmission functions. This would require either some irregular shape of the closing edge of at least the faster chopper window or a gradient in thickness of the absorber material on the chopper disks. The performance of the double chopper system foreseen for the ESS test beamline has been simulated with the neutron ray-tracing program VITESS [27]. The simulation results are compared to the time structure of the ESS pulse in Fig. 3.

Both chopper discs of the double chopper have a diameter of 700 mm in line with the spatial restrictions at their position 21.7 m downstream the cold source. The slower chopper runs at the future ESS source frequency of 14 Hz and has a single window of 23° while the second, counter rotating chopper is operated at 3 times the source frequency, i.e. at 42 Hz and has a window of 50° (see Fig. 3 left). The simulation results presented in Fig. 3 demonstrate, that at least the rising edge and the plateau of the ESS pulse structure are well mimicked that way, while the decay with its relatively long tail is only linearly approximated. Being equipped with such a chopper system the beamline can be used to test systems with a neutron pulse comparable to that of the future ESS.

In addition, a frame overlap chopper is required and will be installed in order to separate pulses at any possible measuring position from 46.17 m to 60 m from the cold source, i.e. between 24.5 m and 38 m from the source pulse chopper system. Accordingly, wavelength bandwidths between 6.1 Å and 10.2 Å width are available within the repetition time. This frame overlap chopper, i.e. the wavelength band defining chopper (WBC), is a double chopper system as well. It allows selecting different

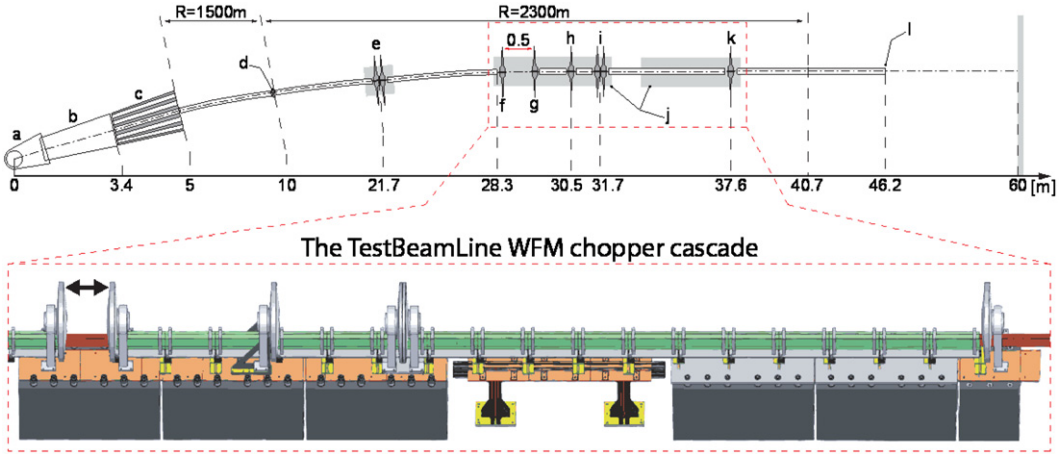

Fig. 1. Schematic view of the guide system installed at HZB and the planned chopper cascade for WFM of the ESS test beamline: (a) cold source moderator, (b) in-pile part, (c) rotary shutter, (d) beamline shutter, (e) ESS source chopper (double), (f) WFM PSC1, (g) WFM PSC2, (h) frame overlap chopper (FOC) 1, (i) wavelength bandwidth chopper (WBC) (double), (j) concrete supports, (k) FOC2, and (l) guide end at 46.2 m distance to the cold source.

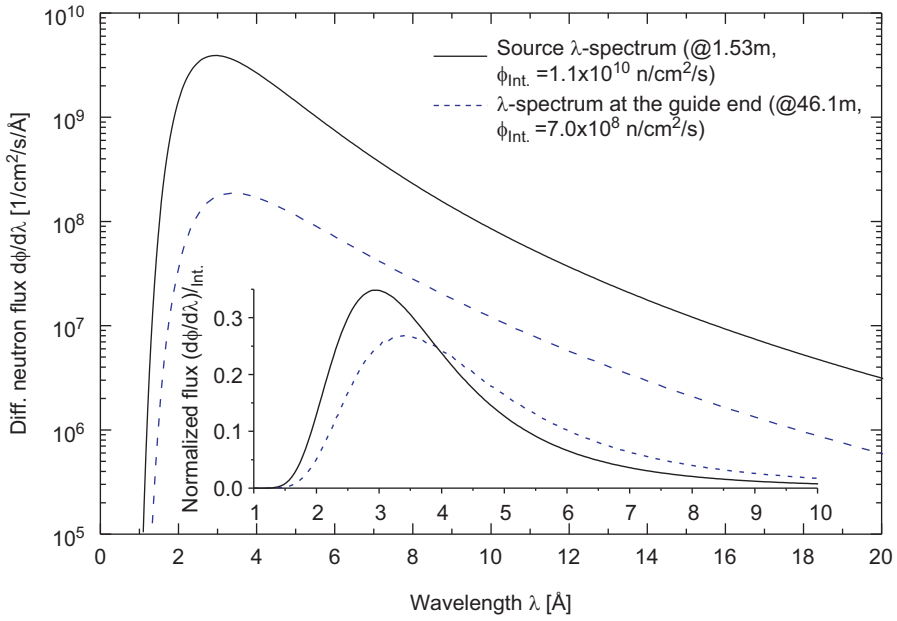

Fig. 2. Simulated differential neutron flux density $d\Phi/d\lambda$ at the in-pile entrance and at the end position of the guide system of the ESS test beamline. The inset shows the same spectra normalized by the total neutron flux density $\Phi_{Int.}$.

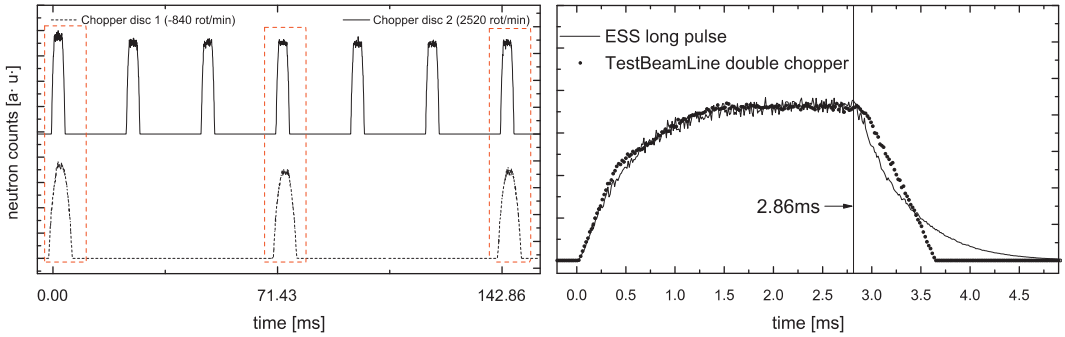

Fig. 3. Left: opening profiles of the two counter rotating chopper discs of the ESS source mimicking choppers. Right: a comparison of the expected ESS pulse shape and the corresponding pulse shape of the test beamline "source choppers".

bandwidths by phasing of the discs. Both discs have a diameter of 700 mm. Chopper 1 has a window of 150° and chopper 2 a window of 202°. Tuning the phase opening times between 0 and 29.8 ms can be chosen. Such basic set-up allows wavelength resolutions defined by the instrument length and the burst time ranging between 23% (11.5%, 5.7%) at 46 m and 14.5% (7.2%, 3.6%) at 59 m for a wavelength of 2 Å (4 Å, 8 Å). For many neutron scattering techniques such as reflectometry, and small angle scattering as well as spin-echo encoding, such wavelength resolution is reasonable.

However, other neutron scattering and neutron imaging methods require better wavelength resolution, which will be realized at the test beamline by means of a wavelength-frame-multiplication chopper system. At the same time this system serves as an experimental test case of a WFM chopper system for future applications at ESS.

2.2. WFM chopper system

Wavelength frame multiplication has been proposed [9–11,21,22] for "white beam" TOF techniques, i.e. techniques using a broad wavelength spectrum simultaneously, in analogy to repetition rate multiplication (RRM) for monochromatizing chopper spectrometers [9,11,21,22,28]. These techniques allow for a more flexible utilization of the pulse structure in particular at long pulse sources via (1) pulse shaping, in order to achieve a desired wavelength resolution at any projected detector distance from the source and (2) multiplexing in order to fill the source repetition time with meaningful neutron counts at the detector. Various simulations and even test measurements underline the practicality of such set-ups at a long pulse source [9–11,21,22,28].

However, while RRM clearly increases the efficiency of spectroscopic measurements at sources with relatively low repetition rate, WFM with a short instrument length is rather an alternative to single frame pulse shaping with a larger instrument length (Fig. 4). WFM is in principle not more efficient in covering a desired wavelength band than alternative solutions. For example two fold wavelength frame multiplication at a given instrument length (Fig. 4a) does fill the detector during the whole source period as well as that of a configuration with two times one half frame at twice the instrument length (Fig. 4b). Note that the latter instrument configuration requires doubling the chopper burst time to achieve the same resolution. A third option with the same principle efficiency is obviously a long instrument utilizing a combination of source pulse suppression and frame multiplication. This configuration can optionally be combined with option

2 and hence would constitute the most flexible set-up able to cover a smaller or a broader scattering vector range (Q-range) simultaneously, depending on the requirements of a specific measurement (Fig. 4c).

Options 1 and 3 are instruments with what is referred to as "natural length" (compare Fig. 4a, c). Their length is defined by the source parameters, the burst time τ and the period T, as well as by the distance of the pulse shaping chopper L_{PS} from the pulsed source by

$$L_{nat} = L_{PS} + L_{PS}T/\tau \quad (1)$$

With length L_{nat} the chopper-shaped neutron pulse fills the whole period T at the detector. For the ESS the closest distance of the first chopper to the source L_{PS} is planned to be 6 m and hence the natural length of pulse shaping instruments is L_{nat}=153 m (note that significant variations occur in length when e.g. double choppers are used and in other cases when the actual L_{PS} varies).

However, there are clearly cases in which WFM at the future ESS source is highly desirable, as instruments require flexible resolutions among which the loosest can be realized most efficiently through the length of the instrument without pulse shaping, but at the same time higher resolutions require WFM in particular when broad wavelength bands are to be covered. For such instruments the test beamline is a test bed. In agreement with such requirements and given the spatial limitations at the test beamline the WFM chopper system has been specified for tunable constant wavelength resolutions dλ/λ of 2% down to 0.5% at 54 m from the cold source (32 m from the source mimicking chopper) for a wavelength band of 7.3 Å starting at 2 Å (cut-off guide system).

The potential to enable tunable but over the wavelength band *constant* wavelength resolutions with pulse shaping choppers at a long pulse source is a big advantage to enable efficient measurements with tailored resolutions and has hence been considered to be established together with a WFM chopper system at the test beamline. This requires combining the approach of WFM with an optical blind chopper system as proposed in Ref. [29] and realized in many modern instruments [15–20] with continuous sources. Note that although wavelength bands can be relatively small, within sub-frames (e.g. 1.5 Å width), especially at the short wavelength side, resolutions might differ up to around 100% between the shortest and longest wavelength of a frame (e.g. 1.5–3 Å) and therefore to the same extent efficiency might vary within a band.

We have investigated the potential to combine constant resolution with WFM by graphical TOF diagrams, which are a

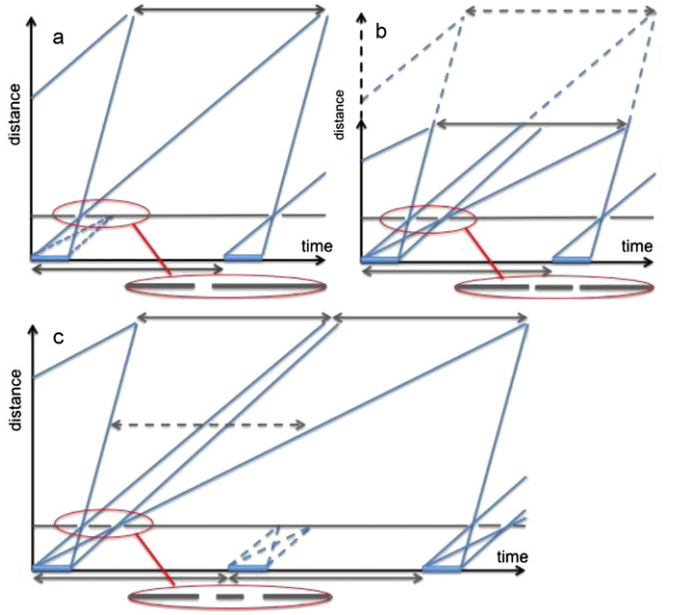

Fig. 4. Schematic TOF sketch of straightforward pulse shaping for a "natural length" instrument: (a) versus 2-fold wavelength frame multiplication at half that length (b) a "natural length" instrument with pulse suppression and (c) underlining the equivalence of all these approaches in terms of efficiency filling the detector with neutrons at all times. Note that in (b) the chopper windows have half the width of that in (a) and (c) in order to achieve the same wavelength resolution at half the instrument length, while (a) just achieves half the bandwidth in one go and (c) suppresses every second source pulse.

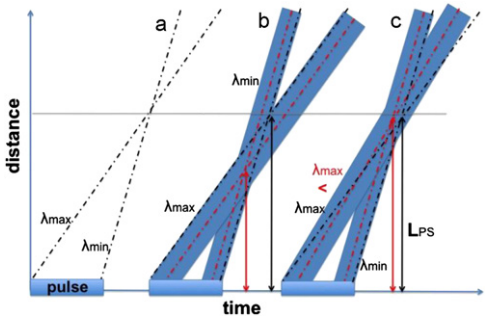

Fig. 5. Schematic TOF sketch visualizing the effect of reduced bandwidth per WFM sub-frame with increasing pulse width. The increase in pulse width may be required either because of reduced resolution needs or longer wavelength at same resolution. As a consequence the mean starting time (dashed line) of the pulse of a specific wavelength shifts towards the middle of the source pulse (b, c). Hence, keeping the band (i.e. angle between the lines defining λ_{min} and λ_{max} in the TOF diagram) constant the pulse shaping chopper(s) would need to be closer to the source (b, red lines), as the efficient source pulse width projected on to the detector position is smaller as seen by the difference in the starting points of the dashed lines. As the chopper(s) have the same position for all subframes and their minimum distance to the source has a lower limit the only solution is to reduce the angular width between the lines (c, red lines), which corresponds to a reduction of the wavelength band with growing pulse widths required for either case, longer wavelength or lower resolution. (For interpretation of the references to color in this figure legend, the reader is referred to the web version of this article.)

Table 1
Chopper specifications for the main WFM chopper system for six-fold frame multiplication and the corresponding wavelength frames.

	Position [m] (from source chopper)	Frequency [Hz]	Window1 [deg.] λ_{min}–λ_{max} [Å] 2–3.45	w2 [deg.] λ_{min}–λ_{max} [Å] 3.45–4.8	w3 [deg.] λ_{min}–λ_{max} [Å] 4.8–6.06	w4 [deg.] λ_{min}–λ_{max} [Å] 6.06–7.23	w5 [deg.] λ_{min}–λ_{max} [Å] 7.23–8.31	w6 [deg.] λ_{min}–λ_{max} [Å] 8.31–9.32
WFMPSC1	28.4; (6.6)	70	10.99	15.3	19.3	23.01	26.46	29.7
WFMPSC2	28.9; (7.1)	70	10.99	15.3	19.3	19.3	23.01	29.68
FOC1	30.5; (8.7)	56	20.64	23.24	21.81	17.87	15.76	24.47
FOC2	37.6; (15.8)	28	36.6	36.06	30.21	26.88	24.56	29.11

helpful tool to specify the chopper parameters for subsequent simulations and allow important conclusions about such a system to be drawn.

Important boundary conditions that had to be taken into account are the spatial constraints, i.e. the maximum length of the instrument of about 60 m with the minimum possible source pulse chopper position at 21.7 m, the requirement to keep the number of choppers as low as possible as well as not being completely free in their positioning due to neighboring beamlines. These practicalities have led to some compromise as is outlined below. A schematic drawing of the beamline providing the most important dimensions is given in Fig. 1, an additional table is provided below (Table 1) while a short description or guidance on how to produce meaningful TOF diagrams in the given case is provided in Appendix A. Here we shall discuss the results and their implications.

One important boundary condition is that in the case of the test beamline the first chopper of the pulse shaping double chopper system cannot be placed at a distance exactly 6 m from the ESS pulse mimicking chopper system. The minimum distance allowing for chopper installation is 6.5 m from the source chopper. In addition for an optical blind double chopper system the TOF starting point is given half way between the first (WFM PSC1) and the second (WFM PSC2) pulse shaping chopper. This further increases L_{PS}. The chopper distance $z_0=L_{PSC2}-L_{PSC1}$ and the distance from the midpoint between choppers PSC1 and PSC2 to the detector $L_{TOF}=L_{Det}-z_0/2$ defines the wavelength resolution $d\lambda/\lambda=z_0/L_{TOF}$. Here L_{Det} is the distance between PSC1 and the detector. Hence for the loosest resolution envisaged, i.e. 2% and the instrument length of 32 m ($L=L_{PSC1}+L_{Det}$), the biggest value z_0 has to be chosen as 0.5 m. Consequently the value of L_{PS} is 6.75 m ($L_{PS}=L_{PSC1}+z_0/2$).

Another consequence of the characteristics of an optical blind double chopper pulse shaping system is that L_{PS} should be kept constant in order to tune the resolution, i.e. changing z_0, at a long pulse source where WFM is used. In turn this requires either moving both choppers along the beam axis [15,16,19] or installing an extra chopper pair for each resolution setting [17,18,20]. Given the spatial constraints and cost-efficiency, only the first option was taken into account for the test beamline at HZB. Consequently the 0.5 m between the two choppers will not be bridged by a neutron guide. Linear stages below the two choppers will allow moving them towards each other to a minimum distance of 12 cm corresponding to a minimum wavelength resolution of 0.5% at the detector position 32 m from the pulse shaping choppers (see Fig. 2). The approach of a movable chopper has been proven successful for an optical blind chopper system for variable resolution at BioRef at HZB already [19].

Having fixed the distance L_{PS} to 6.75 m the number of subframes required to fill the repetition period at the instrument

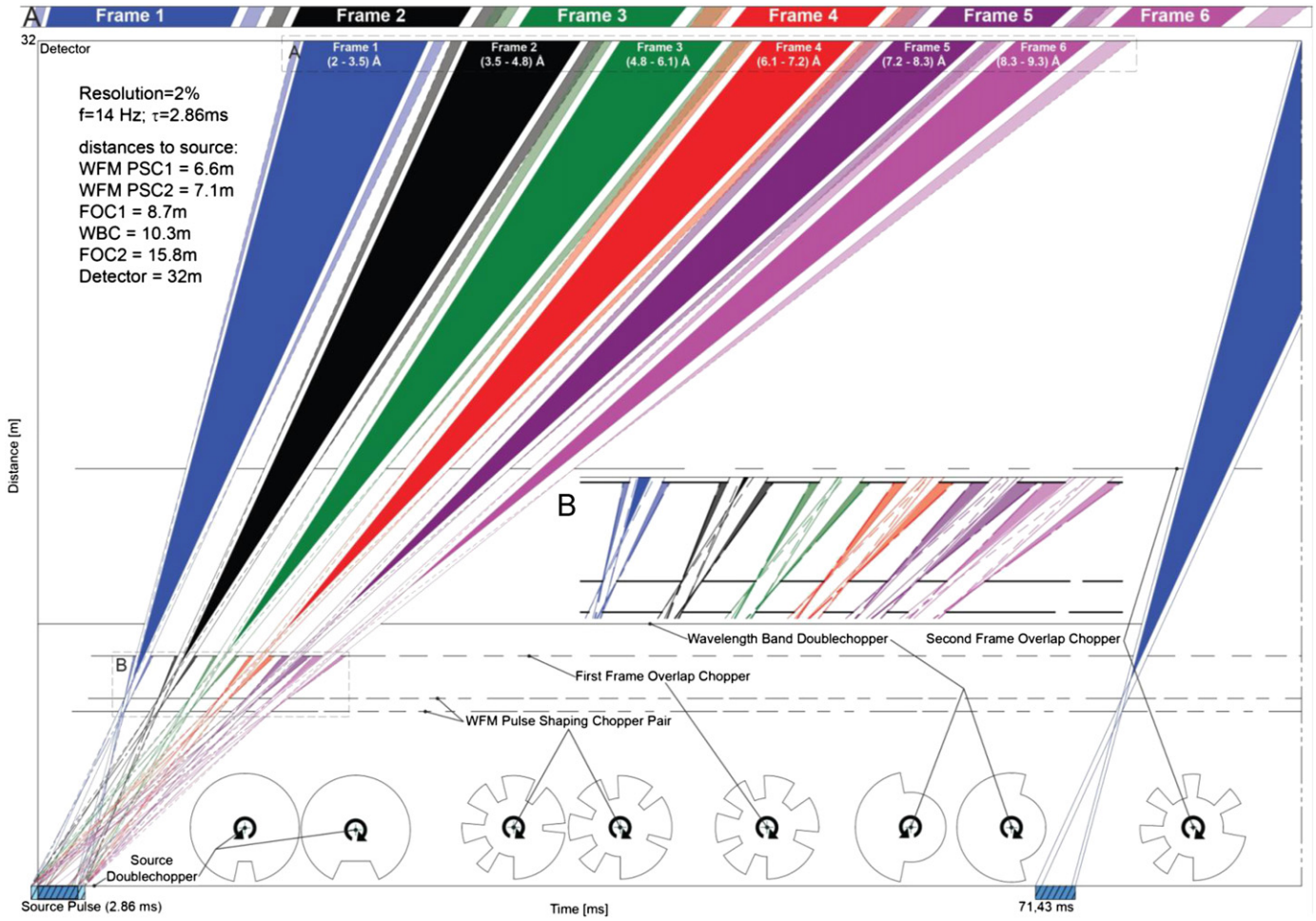

Fig. 6. TOF diagram displaying the chopper set-up as well as the disc profiles; the insets A and B provide magnified views of the detector position and the pulse shaping respectively. The dark colored areas together with the non-colored next to them display the mean of the desired wavelength bands of each sub-frame, while the consecutive semi-transparent areas display potential overlap fractions originating in the pulse blur. These are partly stopped at the frame overlap choppers or otherwise arrive in non-used time fractions at the detector.

length L (source chopper to detector) can be calculated by the ratio of the pulse shaping chopper to detector lengths using the equation

$$N = (L_{nat} - L_{PS})/(L - L_{PS}) = (L_{PS}T/\tau)/(L - L_{PS}) = 6.38 \quad (2)$$

For a future ESS instrument the length can be chosen such that N is an integer number and hence only full frames are taken into account. In the case of the test beamline a number of 6 frames has been chosen in order not having to deal with an additional 38% frame of limited use.

The sub-frames are given by the condition that the shortest wavelength of the $n+1$st sub-frame equals the longest wavelength of the nth frame. Thus the wavelength band is continuously filled (for details see also Appendix A).

However, from the TOF diagrams (Figs. 5 and 6) it can easily be seen that Eq. (2) is a mere approximation, in particular when wavelength resolutions are envisaged, which are close to the "natural wavelength resolution", i.e. close to the resolution achieved using the full source pulse width. In such cases the TOF geometry, which the calculation is based on, holds less and less, because, as illustrated in Fig. 5, the burst time of a certain wavelength moves more and more to the center of the source pulse as the desired burst time becomes comparable to the total source pulse width. Hence, the sub-frames of longer wavelengths significantly decrease in wavelength band and time width and consequently a larger number of sub-frames are required to cover the originally envisaged bandwidth.

A better approximation is therefore to take into account the pulse width for different wavelengths. A straightforward approach is to calculate the "natural length" from a source pulse width reduced by the time resolution of the mean wavelength dt (λ_{mean}) of the desired wavelength band and hence

$$L_{nat} = L_{PS} + L_{PS}T/(\tau - dt(\lambda_{mean})) \quad (3)$$

In case L_{nat} does take into account a chopper system for variable wavelength resolution explicitly, the calculation of L_{nat} should be based on the best wavelength resolution, which corresponds to the broadest wavelength sub-frames. The initial chopper specification of the pulse shaping choppers on the other hand has to be based on the loosest resolution, which requires the biggest chopper openings.

Another important consequence of the fact that the wavelength resolution achieved by pulse shaping approaches the "natural" wavelength resolution at long wavelengths is that the required window sizes of the pulse shaping chopper(s) become large to an extent that the non-window ranges in between become significantly small and hence lead to insufficient sub-frame separation. In such cases when relatively loose wavelength resolutions are required, other than in earlier simulations and instrument proposals of WFM, the window sizes of sub-frame pulses have to be customized with respect to the wavelength frame. This has been done in the case of the test beamline (see Fig. 6 for TOF diagrams and sketches of the layout of chopper disks). On the other hand, this implies however that the rotation frequency of these choppers is severely limited, as windows are distributed over a wide range of the chopper circumference and a limited number of repetitions are possible within one source period.

The limited chopper speed together with limitations in its size, i.e. diameter, due to neighboring beamlines (at HZB as well as at ESS) sets limitations on the beam size that can be chopped with sufficient accuracy in order to realize high wavelength resolutions especially for relatively short wavelengths. In the case of the test beamline the highest demands are given by the envisaged 0.5% resolution for the shortest wavelength of 2 Å. Here calculations and simulations result in a beam width restriction down to 6 mm, whereas it is 25 mm for the case of 2% wavelength resolution (see Fig. 7). At the test beamline this can be achieved by corresponding slit settings only between the two chopper discs, while at future ESS beamlines with similar demands, focusing and defocusing of the beam following the eye-of-the-needle principle [1] are to be considered in particular for the pulse shaping choppers.

Finally, the WFM chopper system requires a number of choppers to avoid frame and sub-frame overlap. Especially the multiple opening of all windows of the pulse shaping choppers, due to their frequency being several times the source frequency in order to increase the cutting accuracy, also has to be taken into account. For the test beamline and its limited length, TOF diagram analysis revealed that only two sub-frame overlap choppers and the frame overlap chopper described above are sufficient to avoid any overlap in principle. Only in the long wavelength range it was necessary to limit one sub-frame slightly more, but not to an extent that would compromise overlap of sub-frames in terms of the wavelength range covered. This seems essential for subsequent stitching of data from single sub-frames, and hence for successful data analysis. Also the sub-frame overlap choppers are designed to operate with multiples of the source frequency as

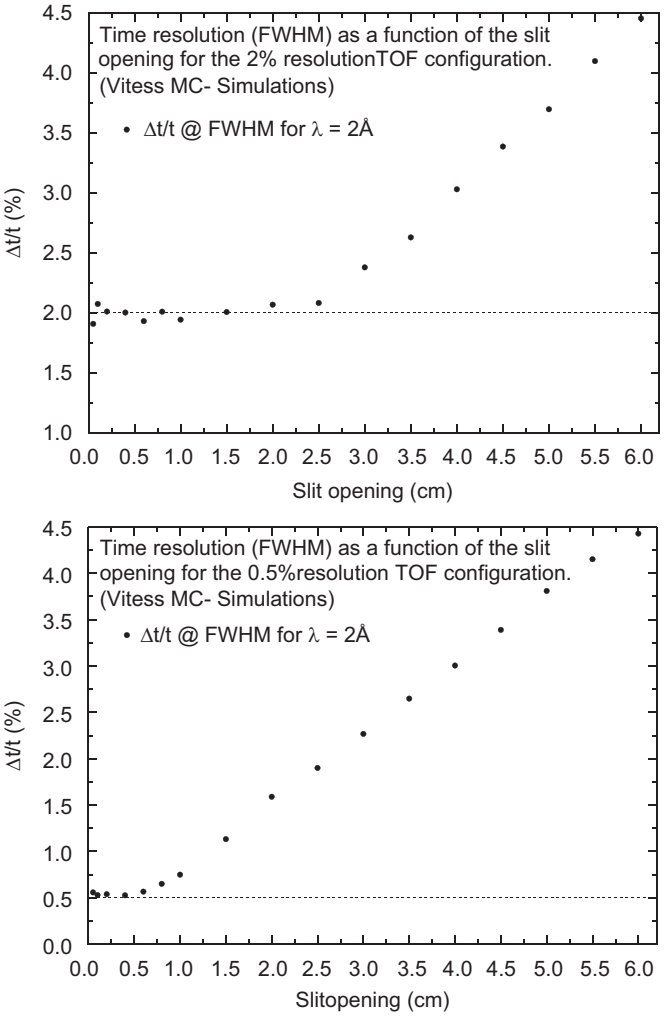

Fig. 7. Simulation of time resolution (burst time at pulse shaping choppers over TOF) for the shortest wavelength used , i.e. 2 Å, as a function of the beam width at the chopper position as defined by a slit between the two pulse shaping choppers for a nominal resolution defined by the chopper distance and the distance to the detector of 2% (left) and 0.5% (right). The results imply that the beamwidth has to be limited to 2.5 cm and 0.6 cm at the chopper pair, in order to reach the nominal resolution for the shortest used wavelength.

shown in the TOF diagrams in Fig. 6 for both limiting resolution cases.

However, simulations revealed, that for the relatively large cross-sections of the actual guide system the chopper parameters did not allow avoiding contaminating overlap between the sub-frames. As the guide cross-section for the test beamline was fixed at the time of the design of the chopper system, overlap had to be avoided by simply introducing slits at three chopper positions, namely $5 \times 10\ \mathrm{cm}^2$ between WFM PSC1 and WFM PSC2 and at the 1st frame overlap chopper and $2 \times 10\ \mathrm{cm}^2$ at FOC2. Additionally, sub-frame overlap chopper windows have been adapted, i.e. reduced slightly (15% for sub-frames 4 and 5, 7.5% for sub-frame 6). Optimization has been carried out in order to avoid the overlap of the sub-frames in the wavelength domain but allowing for maximum possible transmission (see attachment b). These adaptations reduced the flux at the end of the guide to about 25% compared to the system specified by TOF diagrams alone.

Based on the above considerations, and the TOF diagrams as well as analytical calculations and simulations the chopper system has finally been specified as given in Table 1.

All choppers of the WFM system have diameters of 0.6 m. The window sizes are based on a 2% wavelength resolution, because this case requires the largest windows. This window size does not compromise the performance of the system at better resolution settings.

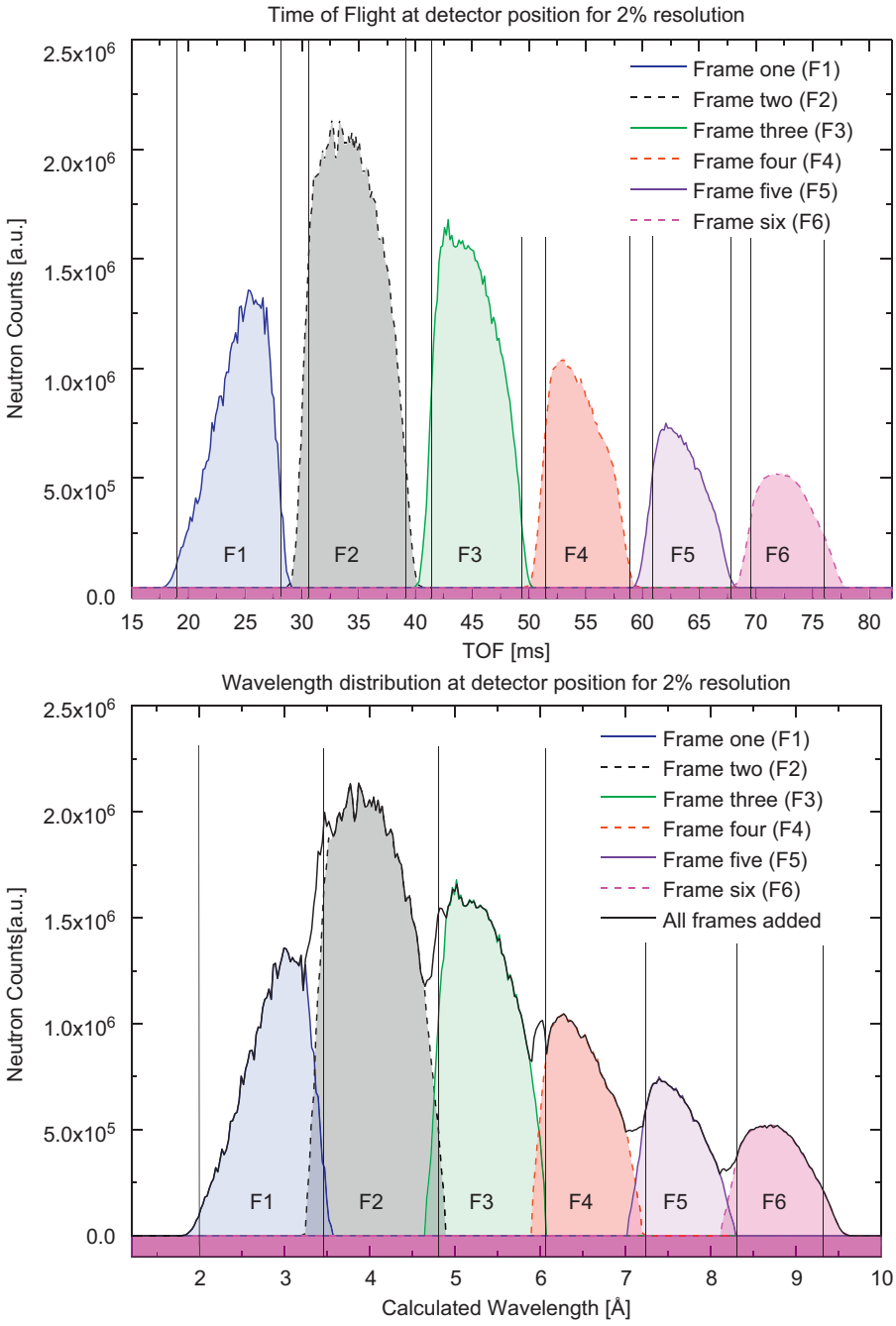

Fig. 8. Results of the simulations for 2% wavelength resolution which show that the sub-frames are sufficiently separated in their arrival time at the detector (top) and at the same time sufficiently overlapping in wavelength range in order to cover the full bandwidth by stitching sub-frames together (bottom). The lines in the diagrams mark the corresponding positions of equal wavelength of subsequent frames; regions containing overlap, i.e. no unique TOF to wavelength solution are cut out and not used in the lower diagram.

2.3. Simulations

Simulations performed with the Monte Carlo ray tracing package VITESS [27] for neutron instrument simulation additionally prove that the sub-frames defined by the chopper system outlined above are well separated in arrival time at the detector. They also well overlap in terms of wavelength, just like desired in order to allow unambiguous mapping of the data to definite wavelengths. The results of such simulations are depicted in Fig. 8. Such an operation mode consequently provides the possibility to either treat data frame by frame and stitch the reduced data or final results or stitch the raw data and process the combined data set subsequently.

3. Summary and discussion

Summarizing, the test beamline at HZB has been designed to provide a time structure close to the ESS long pulse and enable measurements over a wide range of wavelength resolutions from 0.5% to 2% with constant resolution over a wavelength band from 2 Å to 9.5 Å. Also constant resolutions of 4–1% can be achieved in WFM mode if a detector position closer than 32 m is chosen. Without WFM the resolution is wavelength dependent and worse than 3.6% for wavelengths shorter than 8 Å and available for bands of 6.1 Å–10.2 Å width.

Additionally, analytical considerations and the specification of the chopper system for the test beamline demonstrate that it is indeed possible to set up a chopper system for variable constant resolution in a WFM mode at a long pulse source like the ESS. Such a system does not require an excessive number of choppers and provides wavelength frames which are well separated in TOF but at the same time well overlapping in terms of wavelength and should hence allow for efficient data treatment and analyses.

However, the development of the chopper system has revealed several points that have to be kept in mind when designing such a system: (1) the pulse shaping choppers require individual windows for individual wavelength sub-frames in order to realize constant and even medium wavelength resolution, (2) as a consequence chopper frequencies are limited due to the number of different windows required, which (3) impacts (particularly when the chopper size is limited) the size of the beam that can be chopped with the required accuracy. (4) Furthermore, the bandwidth of sub-frames decreases with increasing wavelengths. The latter effect is most significant for wavelength resolutions close to the natural resolution which is given by the source burst time and the instrument length. Here it is important to note that if the natural resolution exceeds the required resolution above a certain, but still required wavelength, additional, for such resolution customized choppers would need to be implemented with a relatively large last window to accept the full pulse for the longest wavelengths required. And last but not the least (5) it was found that avoiding contaminating overlap between sub-frames in the WFM mode strongly depends on the beam size that can be chopped accurately and counter measures like reducing guide cross sections and/or chopper windows have to be taken into account and optimized carefully in order to avoid excessive flux losses.

Finally, such chopper systems are considered most suitable for neutron reflectometry and multi-purpose neutron imaging, as both instruments can make use of a wide range of resolutions. Such instruments profit from quite low resolutions achievable by using the source burst time and a relatively short instrument length providing a broad wavelength range, but require WFM to tune the resolution when needed. Instruments working with lowest resolutions better than that given at the so called natural length of an instrument seem to be more flexible without WFM at shorter length solutions.

Acknowledgment

This work has been supported by the German BMBF under 'Contributions of the Helmholtz Association Centres and Technische Universität München to the ESS Design Update Phase', Förderkennzeichen 05E10CB1.

Appendix A

We outline a systematic graphical approach to designing a chopper system with WFM and constant resolution based on TOF diagrams. Fig. A1–A4.

Note that the chopper discs can have large windows, which does not influence the performance of the chopper pair with respect to the wavelengths under consideration as long as WFM PSC1 closes when WFM PSC2 opens. Consequently, the windows are defined for the lowest resolution case, as higher resolutions require less distance between the two choppers and hence would require smaller windows. Note that such a system in a WFM mode at a pulsed source requires both choppers to move and hence to keep their mean distance from the source constant in order not to change the WFM TOF geometry.

Following the steps outlined above the wavelength frame and chopper parameters can be retrieved geometrically as they are defined by the source pulse (definition) and the corresponding choice of distances and lowest wavelength $\lambda_{\min}$.

It should also be mentioned that the distance between the optical blind operated pulse shaping choppers defines the wavelength resolution together with the distance from half way between them to the detector [29]. Subsequent WFM frames are drawn in the same way and by defining the lowest wavelength of a frame as being equal to the longest wavelength of the previous

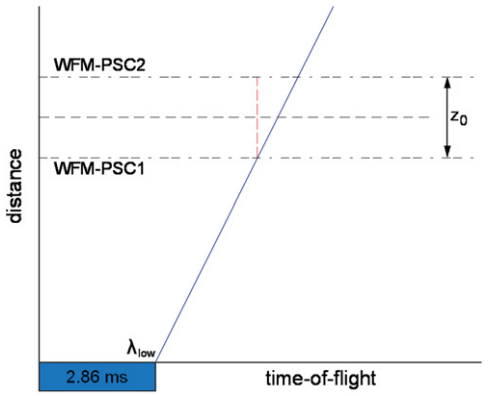

Fig. A1. First the lowest desired wavelength has to be defined as well as the position of the first WFM PSC (WFM PSC1). In the TOF diagram the chopper position is represented by a horizontal line. The wavelength defines the inclination of the corresponding line representing such wavelength in the TOF diagram. For this graphical approach the line for the shortest desired wavelength originates from the latest point in time of the neutron pulse, which is intended to contribute to the system. In the given case it is 2 Å neutrons at 2.86 ms (the nominal pulse width at ESS). The intersection of this line with the first WFM chopper position line (horizontal) defines the closing point of the first WFM pulse shaping chopper (WFM PSC1). From this intersection point a vertical line to the second WFM pulse shaping chopper position, which is defined by the desired wavelength resolution and the length of the instrument [29] (horizontal line), is drawn (red line) which defines the opening point of the second WFM pulse shaping chopper (WFM PSC2). (For interpretation of the references to color in this figure legend, the reader is referred to the web version of this article.)

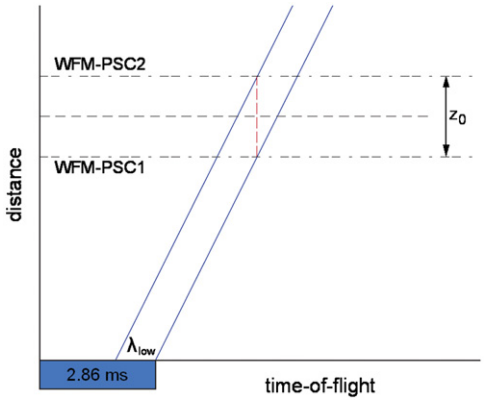

Fig. A2. As the opening point of WFM PSC2 is defined by the vertical line between the two chopper positions the second line for the same wavelength (λ_{min}) defining the pulse width for this wavelength can be drawn which of course has the same inclination (i.e. wavelength) and is hence parallel to the first line. By the intersection point (the opening point of the second chopper) and the fixed inclination this line is fully defined. These lines represent the pulse width defined by the chosen chopper distance of the lowest wavelength λ_{min} of the sub-frame as initially chosen.

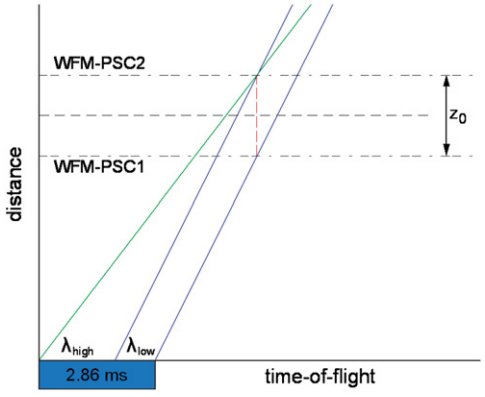

Fig. A3. On the other hand the longest desired wavelength of the corresponding frame (λ_{max}) is now determined by the start of the source pulse (time zero, or any other minimum time chosen as the earliest time to contribute to the instrument) and the opening point of WFM PSC2. This line which represents the lower time limit of the λ_{max} pulse width can be drawn by connecting these two points. The wavelength λ_{max} is defined by the inclination of this line and hence depends on the choice of the chopper distances, the chosen minimum wavelength and the assumed starting and end points of the source pulse.

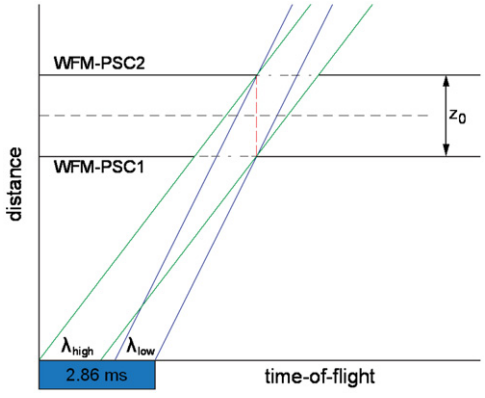

Fig. A4. Intersection of the longest wavelength with the position (horizontal line) of the WFM PSC1 defines the required opening time of this chopper (as the closing point is already defined). The drawing is completed by a line for the longest wavelength intersecting WFM PSC1 at the closing point, and hence also WFM PSC2 at the closing point.

frame. Consequently this way the pulse shaping chopper system can be specified geometrically in a straightforward way.

Appendix B

For WFM to be employed reasonably it is indispensable to avoid frame overlap (FOL) in terms of TOF, while at the same time guaranteeing frame overlap in terms of wavelength ranges of the subsequent wavelength frames (subframes). However, designing the chopper system on the basis of TOF diagrams is not sufficient in this respect, because the diagrams do not take into account the finite beam size and the limited chopper performance concerning opening and closing times. Hence these contamination effects of the real system are best examined by other means like simulations which were used to refine the specifications derived from the TOF diagrams.

The first simulation, the results of which are provided in Fig. B1, resembles the conditions of the TOF diagrams by choosing an extremely small cross-section (0.05 cm in the direction of chopping) of the beam as well as zero divergence. In accordance to the TOF diagram the first three subframes are well separated in time-of-flight and the subsequent subframes (Frames 3–6) show slight overlaps between the subframes only in their penumbrae, which are, however, not required for data collection.

In order to simulate a system like that derived from the TOF diagrams but to see the full influence of real conditions, the divergence in the subsequent simulation is defined by the shape of the in-pile part of the HZB cold neutron source and realistic guide cross sections are implemented in the simulation (Fig. B2). Severe frame overlap is present and would not allow for using the beamline efficiently in WFM mode with the corresponding specifications. Hence, a solution had to be found to avoid these effects closely related to the beam cross-section and the related chopping accuracy.

A first attempt and test of consequences in order to reduce frame overlap was to just reduce the chopper window sizes. An exemplary result of such an approach is shown in Fig. B3. Here the windows for the subframes 3–5 of the FOC1 and FOC2 were reduced symmetrically by 15% of their size. The chopper windows for the subframe number 6 were reduced by 7.5%. As a result the frame overlap problem was reduced but not eliminated. However,

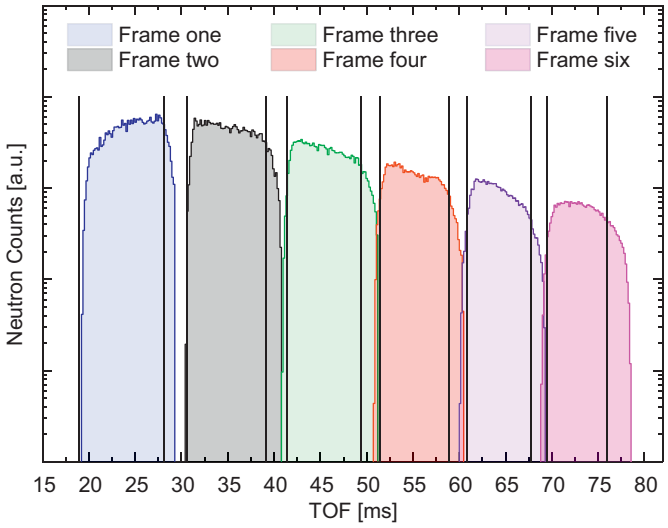

Fig. B1. Zero divergence, one slit between WFM PS choppers with 0.05 cm × 10 cm window.

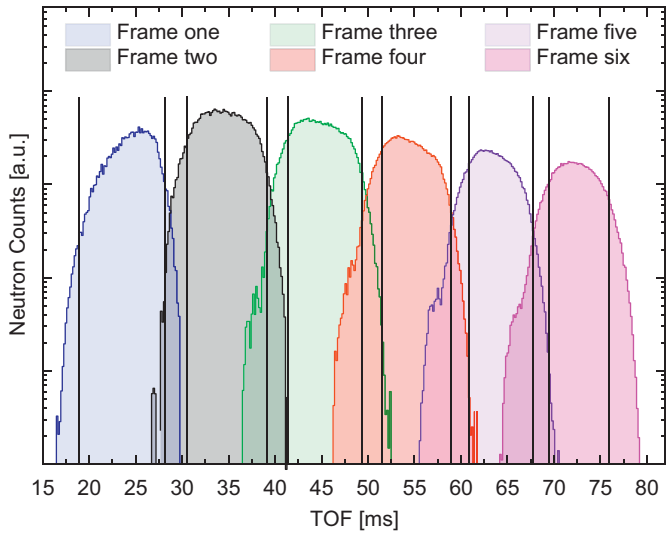

Fig. B2. Divergence defined by the in-pile part geometry; one slit between WFM choppers with 3 cm × 10 cm window.

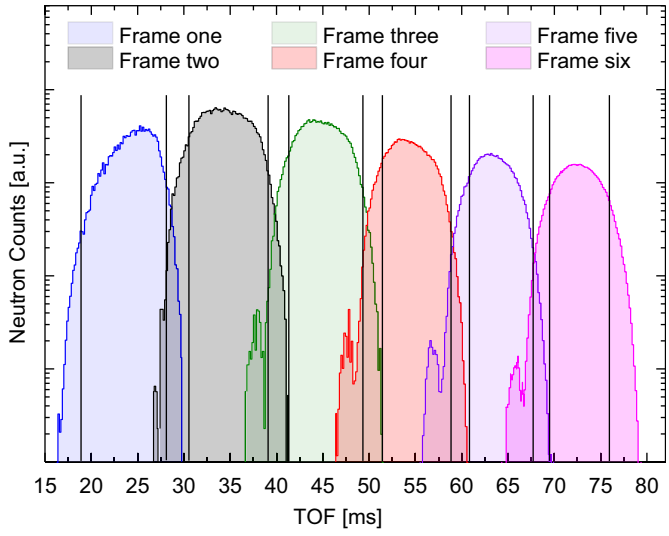

Fig. B3. Divergence defined by the in-pile part geometry; one slit between WFM pulse shaping choppers with 3 cm × 10 cm window; frame overlap chopper 1 and 2 windows were reduced by 15% (subframes 3–5) and 7.5%, respectively (subframe 6).

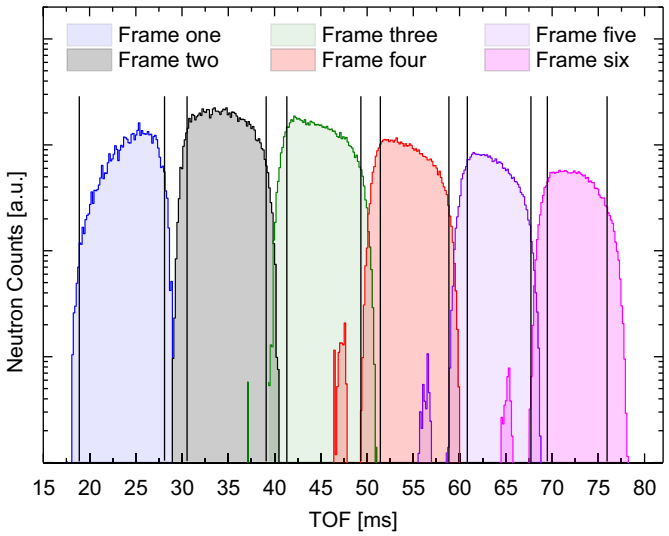

Fig. B4. Divergence defined by the in-pile part geometry; three slits, between WFM-PS-choppers with 5 cm × 10 cm, in front of the FOC 1with 5 cm × 10 cm and in front of FOC 2 with 2 cm × 10 cm windows.

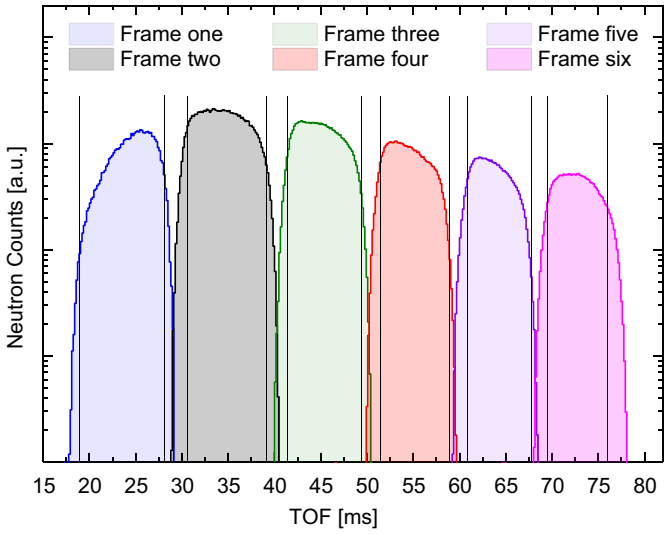

Fig. B5 Final configuration; divergence defined by the in-pile part geometry; three slits, between WFM PS-choppers with 5 cm × 10 cm, in front of FOC 1 with 5 cm × 10 cm and in front of FOC 2 with 2 cm × 10 cm windows; FO chopper 1 and 2 windows were reduced by 15%, respectively (subframes 3–5) and 7.5% (subframe 6).

such an approach also limits the wavelength bands of the subframes and further reduction of the chopper windows would induce significant discontinuity of the wavelength band covered by the WFM.

Hence, another measure had to be taken into account, which naturally involved reducing the beam cross-section at the chopper positions. Again here in order to be able to evaluate the effects of single measures, first the chopper windows were set back to their original sizes derived from the TOF diagrams, and then several slits have been introduced in front of the corresponding choppers. An example of such simulation is given in Fig. B4, where, in addition to the 5 cm × 10 cm slit between the WFM pulse shaping choppers, windows of 5 cm × 10 cm and 2 cm × 10 cm were set in front of FOC1 and FOC2, respectively. Again with this approach it was found that the FO problem was reduced but not sufficiently eliminated. In comparison to Fig. B3 FO "islands" appear in neighboring subframes. A severe drawback of using slits is indeed a significant reduction of neutron flux due to the decreased beam width at several positions. This is especially the case at the test beamline, as the guide geometry was fixed and no eye-of-the-needle concept could be realized (due to cost and time-line) for the moment.

Starting from this point simulations were used to optimize the system according to the findings with a combination of reduced chopper window sizes and slit configurations, in order to fully avoid contaminating frame overlap, while at the same time achieving a continuous spectrum and maximum possible neutron flux. Fig. B5 (partly resembling Fig. 8 in the manuscript) displays the result of such optimization which involves a combination of the above described measures concerning slits and chopper window sizes. The resulting wavelength spectrum covered this way through WFM is provided as well.

References

[1] F. Mezei, Proceedings of ICANS-XII, Abingdon, 1993, RAL Report no. 94-025, I-137.
[2] ⟨http://ess-scandinavia.eu/about-esss⟩.
[3] ESS Project, vol. 4, ESS Council, 2002.
[4] ⟨www.ill.eu/fileadmin/users_files/Other_Sites/YellowBook2008CDRom/index.htm⟩.
[5] ⟨http://www.frm2.tum.de/en/technik/reactor/index.html⟩.
[6] ⟨http://neutrons.ornl.gov/facilities/HFIR/⟩.
[7] ⟨http://neutrons.ornl.gov/facilities/SNS/⟩.
[8] Masatoshi Arai, Fujio Maekawa, Nuclear Physics News 19 (4) (2009) 34.
[9] F. Mezei, Instrumentation concepts: advances by innovation and building on experience, The ESS Project, New Science and Technology for the 21st Century, vol. II,, ESS Council, Juelich, Germany, 2002. (Chapter 3).
[10] K. Lieutenant, F. Mezei, Journal of Neutron Research 14 (2006) 177.
[11] F. Mezei, Comptes Rendus Physique 8 (2007) 909.
[12] M. Russina, Gy Káli, Zs Sánta, F. Mezei, Nuclear Instruments and Methods in Physics Research Section A 654 (1) (2011) 383.
[13] M. Russina, F. Mezei, G. Kali, Journal of Physics: Conference Series 340 (2012) 012018.
[14] H. Schober, et al., Nuclear Instruments and Methods in Physics Research Section A 589 (2008) 34.
[15] M. Gupta, T. Gutberlet, J. Stahn, P. Keller, D. Clemens, Pramana - Journal of Physics 63 (1) (2004) 57.
[16] R. Kampmann, M. Haese-Seiller, V. Kudryashov, B. Nickel, C. Daniel, W. Fenzl, A. Schreyer, E. Sackmann, J. Rädler, Physica B 385 (2006) 1161.
[17] M. James, A. Nelson, A. Brule, J.C. Schulz, Journal of Neutron Research 14 (2006) 91.
[18] C.D. Dewhurst, Measurement Science and Technology 19 (3) (2008) 034007.
[19] M. Strobl, et al., Review of Scientific Instruments 82 (2011) 055101.
[20] R.A. Campbell, H.P. Wacklin, I. Sutton, R. Cubitt, G. Fragneto, European Physical Journal Plus 126 (2011) 107.
[21] F. Mezei, Journal of Neutron Research 6 (1997) 3.
[22] F. Mezei, M. Russina, Advances in neutron scattering instrumentation, in: I.S. Anderson, B. Guerard (Eds.), Proceedings of the SPIE, vol. 4785, 2002, p. 24.
[23] H.A. Graf, D. Clemens, O. Prokhnenko, H.-J. Bleif, C. Pappas, S. Welzel, T. Krist, K. Habicht, M. Russina, Neutron News 20 (2009) 16.
[24] M. Skoulatos, K. Habicht, Nuclear Instruments and Methods in Physics Research A647 (2011) 100.
[25] U. Keiderling, A. Wiedenmann, Physica B 213–214 (1995) 895, V4.
[26] ESS Project, vol. 4, ESS Council, 2002.
[27] ⟨http://www.helmholtz-berlin.de/forschung/grossgeraete/neutronen streuung/projekte/vitess/index_en.html⟩.
[28] Margarita Russina, Ferenc Mezei, Nuclear Instruments and Methods in Physics Research Section A 604 (3) (2009) 624.
[29] A.A. van Well, Physica B 180–181 (1992) 959.